Additive Manufacturing Letters 6 (2023) 100154

Contents lists available at ScienceDirect

Additive Manufacturing Letters

journal homepage: www.elsevier.com/locate/addlet

Short Communication

Fatigue crack propagation in AA5083 structures additively manufactured via multi-layer friction surfacing

Zina Kallien[a,*], Christian Knothe-Horstmann[a], Benjamin Klusemann[a,b]

[a] Helmholtz-Zentrum Hereon, Institute of Materials Mechanics, Max-Planck-Straße 1, Geesthacht 21502, Germany
[b] Leuphana University Lüneburg, Institute for Production Technology and Systems, Universitätsallee 1, Lüneburg 21335, Germany

ARTICLE INFO

Keywords:
Multi-layer friction surfacing
Additive manufacturing
Solid state layer deposition
Fatigue crack propagation
Aluminum

ABSTRACT

Multi-layer friction surfacing (MLFS) is a layer deposition technique that allows building structures from metals in solid state. As approach for additive manufacturing, the re-heating during subsequent deposition processes is significantly lower compared to fusion-based techniques. Available research work presents promising properties of MLFS structures from aluminum alloys, reporting no significant directional dependency in terms of tensile strength. The present study focuses on the fatigue crack propagation behavior and the role of layer-to-substrate (LTS) as well as layer-to-layer (LTL) interfaces. Compact tension specimens were extracted in different orientations from the MLFS stacks built from AA5083. The crack propagation parallel and perpendicular to the LTL interfaces as well as from the substrate material across LTS interface into the MLFS deposited material was investigated. The results show that LTL interfaces play no significant role for the crack propagation, i.e. specimens with LTL interfaces perpendicular and parallel to the crack presented no significant differences in terms of their fatigue crack propagation behavior. The specimens where the crack propagated from the substrate material across the LTS interface into the MLFS deposited material showed higher fatigue life than the specimens with crack propagation in the MLFS deposited material only. Crack retardation can be observed as long as the crack propagates within the substrate material, which is associated with compressive residual stresses introduced in the substrate during the layer deposition process.

1. Introduction

The layer-by-layer building of a structural part, i.e. additive manufacturing (AM), combines advantages as flexibility with high degree of freedom in design for near-net-shape geometries [1] with minimum post-processing effort and waste of material [2] compared to subtractive methods. Common AM processes melt a consumable material, i.e. powder or wire, due to the energy input, which solidifies again and manufactures a part with this approach layer by layer, where many metallic materials are shown to be feasible [3].

The fatigue properties as well as the role of layer interfaces for crack propagation behavior is a topic of interest for additively generated structures. For direct energy deposition processes such as for wire-arc additive manufacturing (WAAM) of titanium, Zhang et al. [4] found that the crack propagation rate is affected by the resulting microstructure. For cracks propagating across layers' interfaces, the growth rate was found to be slightly slower compared to cracks propagating along the interfaces [5], where the directional dependency of the microstructural characteristic, i.e. the lamellar structure of the WAAM deposited material, was mentioned as one reason for the different crack propagation rates in the different directions. Defect formation at the interfaces can also have major effects on fatigue properties [6]. The mentioned microstructural characteristics and defect formation affecting the fatigue properties of fusion-based AM parts are strongly related to the thermal history, i.e. heating and cooling cycles as well as re-heating of the structure [7]. Therefore, the effect of post-processing of AM structures on fatigue properties, e.g. via heat treatment [6] or local modification techniques [8], is under investigation. Solid-state AM processes induce a moderate temperature compared to fusion-based processes and many issues related to material melting and solidification can be avoided.

The principle of friction surfacing (FS) was shown to be a potential candidate as solid-state layer deposition technique, i.e. solid-state AM [9]. FS was first mentioned by Klopstock and Neelands [10]. The layer deposition of a consumable material on a substrate below the materials' melting temperatures is enabled by friction and plastic deformation. The FS deposition process can be divided into two phases: First, the plasticizing phase (i) is initiated when the consumable stud material experiences a defined rotational speed and axial force. As a result, the stud is pressed onto the substrate surface, frictional heat is

* Corresponding author.
E-mail address: zina.kallien@hereon.de (Z. Kallien).

https://doi.org/10.1016/j.addlet.2023.100154
Received 28 April 2023; Received in revised form 22 May 2023; Accepted 29 May 2023

generated at the materials' interface and the tip of the stud starts to deform and plasticize. The superimposition of a relative translational movement between substrate and stud material initiates the deposition phase (ii) and enables the deposition of the plasticized consumable material onto the substrate. Layer depositions via FS were investigated for various similar and dissimilar material combinations. An overview is given for instance in the review by Gandra et al. [11]. Apart from potential as solid-state AM technique, which is also focus of the present study, FS also finds potential application as coating [12] or repair [13] technique.

Being a discontinuous process, the dimensions of every FS layer depend on the geometry of the used stud material. Therefore, building one structure from multiple FS layers needs to be investigated in order to allow larger final dimensions independent from the used stud material. The FS process variants of depositing multiple layers adjacent to or on top of each other are known as multi-track friction surfacing (MTFS) and multi-layer friction surfacing (MLFS), where each single layer deposition follows the FS principle. Tokisue et al. [14] performed MTFS with two layers and observed that the tensile strength of the FS deposited material in multiple layers is higher compared to single layer FS. With perspective to MLFS, the FS-characteristic rough surface helps the plasticizing of the subsequent layer deposition on top [15]. MLFS structures with three layer depositions were shown for aluminum on an aluminum substrate [16] and on a steel substrate [17]. A six-layers MLFS stack was built by Shen et al. [18] observing homogeneous microstructure along building direction. Rath et al. [19] built MLFS stacks from up to ten layers in order to extract micro-flat tensile specimens. The results showed no significant gradient along stack length and also no significant directional dependency in terms of tensile strength. Similarly, Kallien et al. [20] extracted tensile specimens, containing MLFS layer material only, from an 18-layers stack. The results confirmed the absence of a gradient in terms of tensile strength along the MLFS stack length at room temperature as well as at elevated testing temperatures. Furthermore, it was shown that the MLFS tensile strength is slightly higher than the base material strength at room temperature. Apart from that, FS has proved the potential and feasibility as solid-state AM technique by combining the FS process variants of MLFS and MTFS, which was shown for steel [9] and aluminum [21]. However, available studies on MLFS hardly provide insights into mechanical properties and especially fatigue crack propagation behavior of MLFS deposited structures are unknown.

Another solid-state AM process, which is closely akin to the FS deposition principle, is additive friction stir deposition (AFSD). Similar to FS, a rotating consumable material is pressed onto a substrate enabling the plasticization. Contrary to FS, AFSD uses a hollow non-consumable tool, which is feeding the consumable material and consolidates the deposited material. Similar to FS, the deposited material presents a refined recrystallized microstructure [22]. For AFSD, some studies on the fatigue properties are available in the literature. For instance, Williams et al. [23] investigated the fatigue properties for AFSD built structures from WE43 magnesium and reported decreased fatigue life compared to feedstock material in the low cycle regime; however, comparable fatigue life was achieved in the high cycle regime. For AA6061 processed via AFSD, Rutherford et al. [24] report homogeneous behavior of the deposited material and mention similar fatigue crack nucleation and growth mechanism like the corresponding AA6061 wrought material. However, similar to MLFS, the fatigue crack propagation behavior is hardly investigated.

This study investigates the fatigue crack propagation behavior of MLFS structures, addressing in particular the influence of the layer-to-substrate (LTS) and layer-to-layer (LTL) interfaces. Furthermore, the present study proves the high repeatability of the MLFS process by, for the first time to the authors' knowledge, showing the successful deposition up to 38 MLFS layers. The built stacks were used to extract specimens in different orientations for the investigation of the fatigue crack propagation (FCP).

2. Materials and methods

2.1. MLFS

A custom-designed friction welding system (RAS, Henry Loitz Robotik, Germany) optimized for FS and related processes was used to build MLFS stacks for this study. The equipment provides the necessary stiffness and repeatability and allows maximum axial force of 60 kN, torque of 200 Nm and rotational speed of 6000 rpm. The FS depositions were performed force-controlled with computer-numerical control (CNC) of the deposition path, which was 200 mm. All processes were executed at room temperature and between the subsequent MLFS layer depositions, the previously deposited material had enough time to cool down to room temperature. A similar material combination was used in this study, the substrate material being AA5083-O (30 mm thickness) and the stud material AA5083-H112 (125 mm length, 20 mm diameter). The process parameters were kept constant at 8 kN axial force, 1200 rpm rotational speed and 6 mm/s travel speed for all layer depositions. The achieved layer thickness with the mentioned process parameters and setup is approx. 1.3 mm. Three stacks were build with 27, 29 and 38 layers in order to provide necessary dimension for the extraction of specimens for FCP testing.

2.2. FCP

Compact tension (C(T)) specimens according to ASTM E647-15 were extracted from the build MLFS stacks. The C(T)50 specimens present a thickness of 5 mm and an initial crack length of $a_0 = 12.5$ mm, Fig. 1(c). Three different types of C(T)50 specimens in the MLFS stacks were analyzed in the investigation, Fig. 1, where two specimens were examined per type. The specimens were extracted at two different orientations, i.e. parallel ($\parallel$) and perpendicular ($\perp$) to the LTL interfaces. Furthermore, in one set of specimens, the pre-crack starts within the substrate material, where its orientation is perpendicular to the LTL interfaces. For the other two types of specimens, the crack starts within the MLFS deposited material. For comparison purpose, two additional C(T)50 specimens were taken from an AA5083-H111 sheet, representing the reference material. The two specimens were extracted from different orientations, Fig. 2, i.e. reference(1) specimen presents the initial crack perpendicular to the sheet's rolling direction and the reference(2) specimen parallel to it.

The investigation of the FCP was performed at room temperature using a servo-hydraulic testing machine (Instron 8800, Schenck) equipped with a 25 kN load cell. The specimens were tested at constant amplitude loading using a maximum force of 2.525 kN and a stress ratio of 0.1. The crack length, a, was measured via optical microscopy at both sides of the specimen during testing. The crack opening displacement (COD) was measured experimentally at the crack mouth of the initial notch using strain clips. The C(T)50 specimens were tested to a final crack length of 30 mm. Afterwards, the specimens were separated using a tensile testing machine (ZwickRoell, Germany) equipped with a 200 kN load cell at constant speed of 0.5 mm/min. The fracture surfaces were investigated via optical light microscopy (VHX 7000, Keyence).

3. Results and discussion

3.1. MLFS process behavior

The FS process is shown to be highly repeatable also for stacks of up to 38 layers, i.e. the behavior during the deposition process was nearly constant as well as the resulting layers are homogeneous, Fig. 3. In order to investigate the deposition behavior during the FS process and possible trends regarding MLFS, the remaining stud length was measured. The length of the remaining studs after layer deposition does not significantly change for the different stacks built at constant process parameters, Fig. 4. Furthermore, as the deposition processes are performed

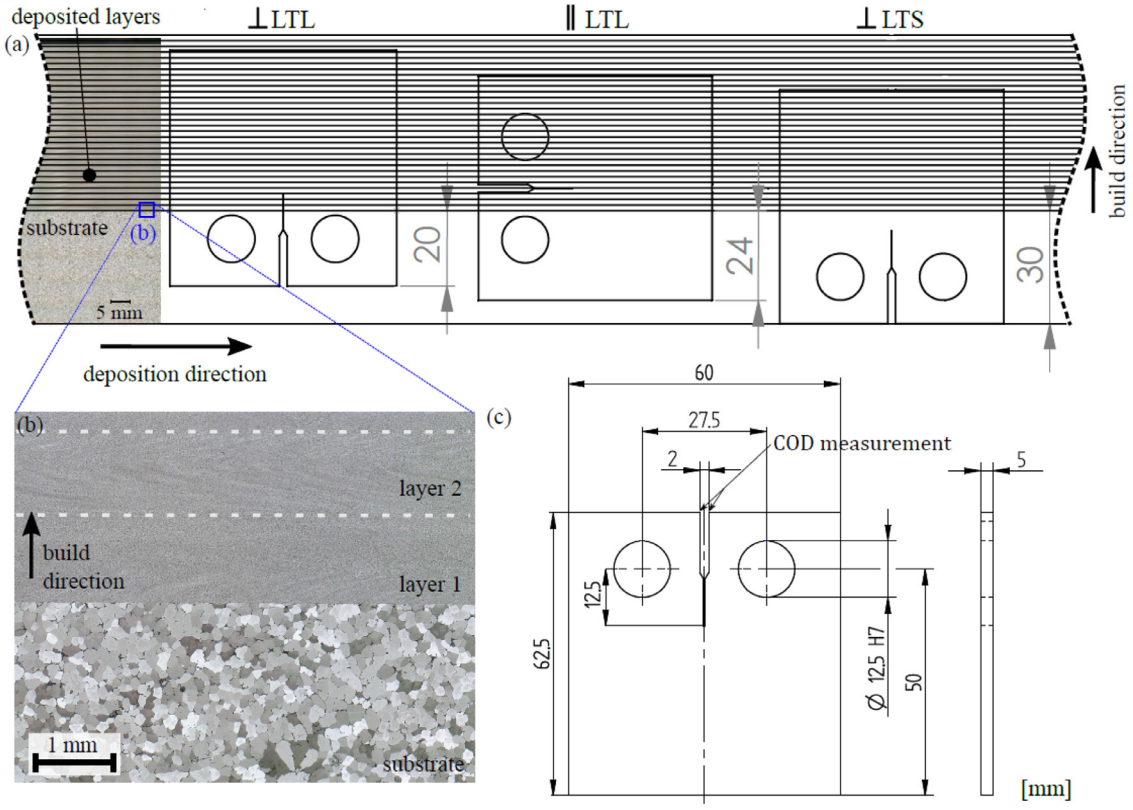

Fig. 1. Schematic positioning of C(T)50 specimens in MLFS stack (a), micrograph of the longitudinal section of the interface between substrate and deposited layers (b) and dimensions of the C(T)50 specimens (c). All dimensions in mm.

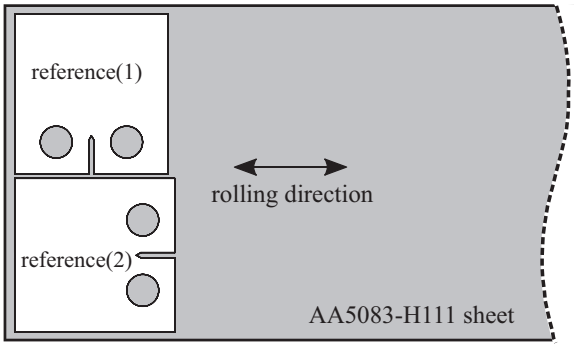

Fig. 2. Schematic positioning of reference C(T)50 specimens in two orientations in AA5083-H111 sheet with respect to the rolling direction.

force-controlled, the resulting stud consumption rate, v_{cr}, is also an indicator in order to evaluate process stability and repeatability. As shown for all layer depositions in Fig. 4, no significant difference or trend can be observed for the stud consumption rate. Overall, the MLFS principle showed a reliable behavior when building high stacks as required for the FCP specimen extraction.

3.2. Fatigue crack propagation

The FCP behavior of the C(T)50 specimens extracted at different orientations within the MLFS stacks is shown in Fig. 5, where the crack starts within the MLFS deposited material parallel (∥LTL) and perpendicular (⊥LTL) to the LTL interfaces. Both tested orientations reached the final crack length of 30 mm after approx. 40 000 cycles, Fig. 5(a), and no significant difference in terms of crack propagation rate could be observed, Fig. 5(c). The reference C(T)50 specimens from the reference sheet material, i.e. reference(1) and reference(2), show a slightly better fatigue performance, where the final crack length was reached after approximately 50 000 cycles, Fig. 5(a). However, the overall FCP behavior is comparable for the MLFS deposited material and the AA5083-H111 reference material. In terms of crack propagation within the MLFS material, the crack paths, Fig. 6(a) and (b), show a straight crack propagation for cracks parallel and perpendicular to LTL interfaces, respectively. Especially for ⊥LTL, the observed deflection of the crack path is very small. This leads to the hypothesis that the LTL interfaces do not have a signif-

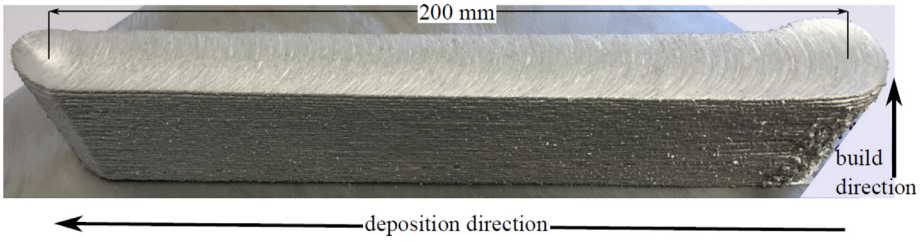

Fig. 3. MLFS stack built from 38 layers at 8 kN, 1200 rpm and 6 mm/s.

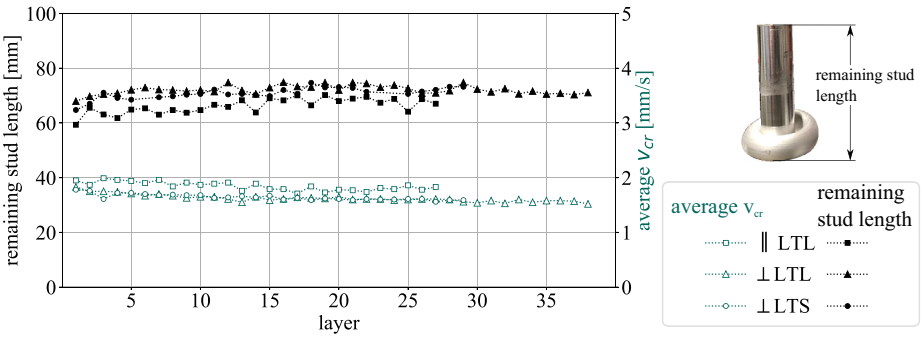

Fig. 4. Average stud consumption rate, v_{cr}, and remaining stud length after 200 mm deposition length for stacks of 27 to 38 layers deposited at constant process parameters of 8 kN, 1200 rpm and 6 mm/s.

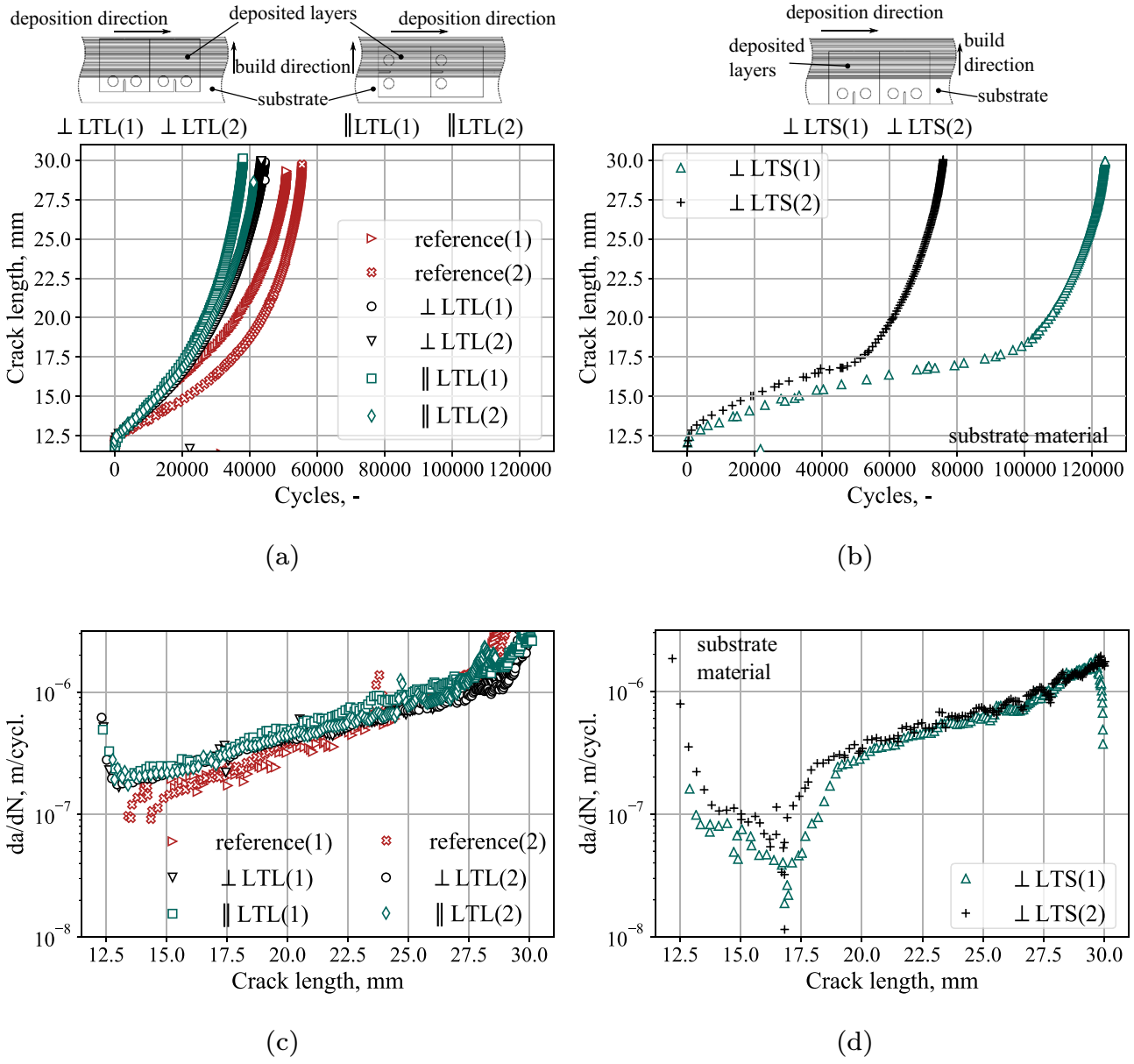

Fig. 5. Crack length over number of cycles for C(T)50 specimens with crack propagation within MLFS deposited material parallel and perpendicular to layer interfaces as well as within reference material (a) and with fatigue crack propagation across LTS interface (b); da/dN over crack length for crack propagation within MLFS deposited material parallel and perpendicular to layer interfaces (c) and with crack propagation across LTS interface (d).

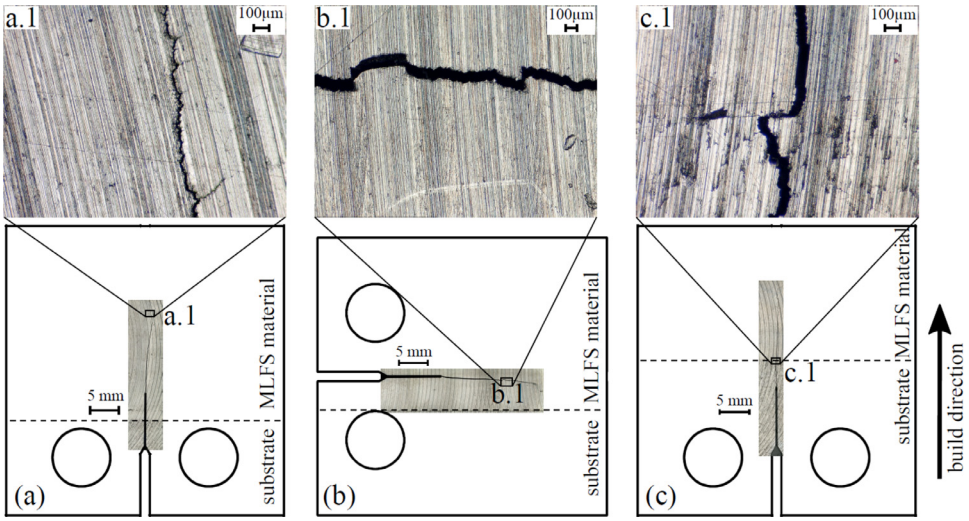

Fig. 6. Crack paths of tested C(T)50 specimens taken from MLFS stacks, propagating perpendicular to LTL (a), parallel to LTL (b) and from substrate into MLFS deposited material, perpendicular to LTS/LTL (c).

icant effect on the fatigue crack propagation within the AA5083 MLFS deposited material. The corresponding fracture surfaces, Fig. 7(a) and (b), show a very homogeneous appearance, Fig. 7(b.1), however, the exemplary specimen for the ⊥LTL orientation presents some surface defects, Fig. 7(a.1). Overall, the fatigue crack propagation behavior for both orientations is very similar, indicating that the LTL interfaces do not appear to play a detrimental role in terms of mechanical properties, which agrees with findings from static tensile testing [19].

For the third tested specimen type (⊥LTS), the crack started in the substrate material (AA5083-O) and propagated across the LTS interface into the MLFS deposited material. The ⊥LTS specimens showed significantly higher number of cycles until the final crack length of 30 mm was reached, Fig. 5(b), compared to the AA5083-H111 reference material and the specimens with crack propagation within the MLFS deposited material only. Figure 5(d) clearly reveals that the fatigue crack propagation rate is different within the first 5 mm of the crack, i.e. within the substrate material. However, as soon as the crack reaches the LTS interface, the fatigue crack propagation rate is similar to the other tested MLFS samples. At the LTS interface, the crack path shows a reorientation parallel to the interface and then propagates straight within the MLFS deposited material, perpendicular to the LTL interfaces, Fig. 6(c).

The MLFS stack material shows an average grain size between 4 µm and 5 µm, which was determined in previous studies of MLFS for the similar consumable material [18] as well as the same process parameters [19]. This is a significantly finer microstructure for instance compared to AA5083-H111 rolled sheet material, which typically presents a gran size of 30 to 50 µm [25–27] with elongated grains along the rolling direction, or cast AA5083-O with grain sizes larger than 200 µm, Fig. 1(b). An in-depth analysis of the detailed grain size distribution in MLFS stacks along each layer is part of current research. The effect of the coarse (substrate) or fine (MLFS) microstructure is assumed to be negligible for long cracks, i.e. in the 'Paris' regime [28]. Therefore, the differences in the fatigue crack propagation behavior between ⊥LTS and LTL specimens might be related to the two following aspects. On the one hand, these might be correlated with material defects within the deposited material, Fig. 7(a.1), which can be also seen at the LTS interface, Fig. 7(c.2). However, more likely, the observed FCP behavior of the ⊥LTS specimens is associated with the present residual stresses within the substrate. Due to the layer deposition process, i.e. thermo-mechanical input, significant sub-surface compressive residual stresses are introduced into the substrate material, as shown by Dovzhenko et al. [29]. The authors [29] investigated the residual stresses for single layer FS of Ti in combination with fatigue testing, where the FS layer was intended as crack stopper. The FS deposited coating presented tensile residual stresses, where compressive stresses were determined within the substrate, compensating the tensile stresses within the deposit. Within the study [29], it was concluded that the travel speed and the deposit thickness affect mainly the residual stress distribution. An improvement of fatigue properties correlating with the residual stresses was found, however, the underlying effects could not be quantified. Similar results in terms of residual stress distribution for single layer FS deposits were obtained from experiment and simulation by Bararpour et al. [30]. However, the authors [30] also found tensile residual stresses within the coating. Additionally, lower residual stresses were determined on the advancing side than on the retreating side, which was attributed to the asymmetric characteristic of the FS process in terms of heat distribution and material flow. In the current study multiple FS layers are deposited, however, the underlying residual stress distribution is assumed to be similar, i.e. in particular compressive residual stresses are introduced within the substrate underneath the deposited material. Furthermore, the observed fatigue crack retardation within the substrate is very alike to observations for local residual stress modification techniques. For instance, Keller et al. [31] showed that the introduced compressive residual stress field due to laser shock peening leads to a significant retardation effect of the fatigue crack propagation within the peened region. Furthermore, Pouget and Reynolds [32] investigated the fatigue crack propagation for friction stir welded AA2050. The compressive residual stresses in the heat-affected zone were found to induce crack closure leading to improved fatigue properties. Increased crack propagation rate was found in the weld nugget, where tensile residual stresses as well as microstructural characteristic were mentioned as possible reasons. Although both ⊥LTS specimens show a similar FCP behavior, the overall number of cycles is significantly different between them. As the two specimens were taken along the stack length, there might be a gradient in terms of residual stresses in the substrate material along deposition length. The gradient might be related to the plasticizing of the consumable, where the rotating stud is pressed onto the substrate to deform and plasticize. This induces a slight change in the thermo-mechanical input to the substrate plate over the deposition duration. Zhu et al. [33] observed tensile residual stresses at the starting position as well as center along the AA6061 AFSD stack and compressive residual stresses at the end. This residual stress distribution within the stack was attributed to the temperature distribution during the process. Due to an initial dwell time to initiate plasticization of the material to enable layer deposition, more frictional heat was generated at the starting end, resulting in higher temperatures compared to the deposition end.

Overall, the presented results are a first attempt to investigate and understand the role of interfaces for the FCP behavior of MLFS deposited

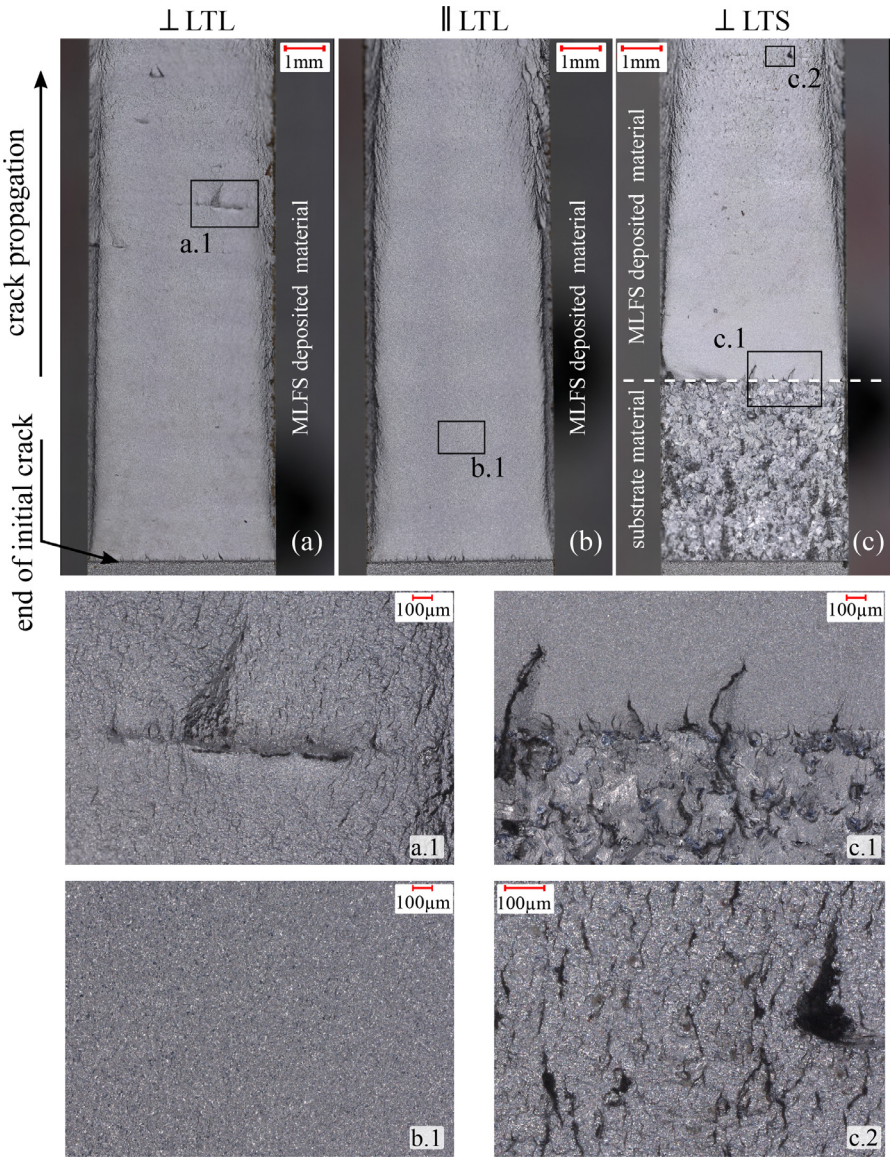

Fig. 7. Fracture surfaces of tested C(T)50 specimens taken from different orientations from the MLFS stacks within crack propagation in the deposited material (a) perpendicular (⊥LTL) and (b) parallel (∥LTL) to LTL interfaces as well as (c) crack propagating from substrate material into MLFS structure (⊥LTS).

structures, applying a constant process parameter set for a similar material combination of a non-precipitation-hardenable aluminum alloy. For sure, a variation of material or process parameters will affect the fatigue properties, as e.g. grain size as well as other microstructural characteristics (grain orientations, size and volume distribution of precipitates in case of a precipitation hardenable alloy, etc.) will be influenced. Although the number of available specimens was limited, all specimens revealed a similar fatigue crack propagation rate for different orientations within the MLFS material indicating no significant effect of LTL interfaces, which is a promising finding. Overall, the FCP experiments underline the homogeneity of the MLFS deposited material, supporting previous findings on static properties [19]. The observed crack retardation for the FCP within the substrate material is of high relevance, especially in view of repair applications.

4. Conclusion

The presented work showed high additive structures achieved via solid-state layer deposition, i.e. MLFS. Up to 38 layers were successfully build, presenting a repeatable process behavior at constant process parameters. In this study, a similar material combination (AA5083) and constant process parameters have been used. C(T)50 specimens were extracted from MLFS stacks with crack tip starting within the substrate material as well as within the MLFS deposited material at different orientations for investigation of the fatigue crack propagation. The main results obtained for the exemplary process parameter set and the deposited non-precipitation-hardenable alloy AA5083 can be summarized as follows:

- MLFS was highly repeatable and stacks of a height up to about 48 mm were achieved with a similar material combination at constant process parameters.
- Layer-to-layer interfaces do not have a significant effect on crack propagation, i.e. no significant difference could be observed for cracks parallel and perpendicular to these interfaces.
- For fatigue crack propagation from substrate material into MLFS deposited material (perpendicular to interfaces), crack retardation can be observed as long as the crack is within the substrate material. This is likely to be related to compressive residual stresses evolved in the substrate material due to the thermo-mechanical input during the MLFS deposition process.

In this regard, the role of the layer-to-substrate interface will be a topic of increased complexity when dissimilar materials are joined. Furthermore, a detailed investigation in order to understand the residual

stress distribution in MLFS deposited structures has to be part of future investigations on this subject.

Funding

This project has received funding from the European Research Council (ERC) under the European Unions Horizon 2020 research and innovation programme (Grant agreement no. 101001567).

Declaration of Competing Interest

The authors declare that they have no known competing financial interests or personal relationships that could have appeared to influence the work reported in this paper.

CRediT authorship contribution statement

Zina Kallien: Conceptualization, Data curation, Formal analysis, Investigation, Methodology, Writing – original draft, Validation, Visualization, Writing – review & editing. **Christian Knothe-Horstmann:** Supervision, Writing – review & editing. **Benjamin Klusemann:** Funding acquisition, Resources, Supervision, Conceptualization, Writing – review & editing.

Data availability

The obtained data of this research is online available at Zenodo (doi:10.5281/zenodo.7983713).

References

[1] W.E. Frazier, Metal additive manufacturing: a review, J. Mater. Eng. Perform. 23 (6) (2014) 1917–1928, doi:10.1007/s11665-014-0958-z.
[2] S. Ford, M. Despeisse, Additive manufacturing and sustainability: an exploratory study of the advantages and challenges, J. Clean. Prod. 137 (4) (2016) 1573–1587, doi:10.1016/j.jclepro.2016.04.150.
[3] D. Herzog, V. Seyda, E. Wycisk, C. Emmelmann, Additive manufacturing of metals, Acta Mater. 117 (3) (2016) 371–392, doi:10.1016/j.actamat.2016.07.019.
[4] J. Zhang, X. Wang, S. Paddea, X. Zhang, Fatigue crack propagation behaviour in wire+ arc additive manufactured Ti-6Al-4V: effects of microstructure and residual stress, Mater. Des. 90 (2016) 551–561,doi:10.1016/j.matdes.2015.10.141.
[5] X. Zhang, F. Martina, A.K. Syed, X. Wang, J. Ding, S.W. Williams, Fatigue crack growth in additive manufactured titanium: residual stress control and life evaluation method development, in: International Comitee on Aeronautical Fatigue ad Structural Integrity 25th Conference and (29th Symposium), ICAF, 2017.
[6] A. Yadollahi, N. Shamsaei, S.M. Thompson, A. Elwany, L. Bian, Effects of building orientation and heat treatment on fatigue behavior of selective laser melted 17-4 PH stainless steel, Int. J. Fatigue 94 (2017) 218–235, doi:10.1016/j.ijfatigue.2016.03.014.
[7] A. Yadollahi, N. Shamsaei, Additive manufacturing of fatigue resistant materials: challenges and opportunities, Int. J. Fatigue 98 (2017) 14–31, doi:10.1016/j.ijfatigue.2017.01.001.
[8] A. Du Plessis, D. Glaser, H. Moller, N. Mathe, L. Tshabalala, B. Mfusi, R. Mostert, Pore closure effect of laser shock peening of additively manufactured AlSi10Mg, 3D Print. Addit. Manuf. 6 (5) (2019) 245–252,, doi:10.1089/3dp.2019.0064.
[9] J.J.S. Dilip, S. Babu, S.V. Rajan, K.H. Rafi, G.D.J. Ram, B.E. Stucker, Use of friction surfacing for additive manufacturing, Mater. Manuf. Process. 28 (2) (2013) 189–194, doi:10.1080/10426914.2012.677912.
[10] H. Klopstock, A.R. Neelands, An improved method of joining or welding metals, 1941,
[11] J. Gandra, H. Krohn, R.M. Miranda, P. Vilaça, L. Quintino, J.F. DosSantos, Friction surfacing—A review, J. Mater. Process. Technol. 214 (5) (2014) 1062–1093, doi:10.1016/j.jmatprotec.2013.12.008.
[12] M. Yu, H. Zhao, Z. Zhang, L. Zhou, X. Song, N. Ma, Texture evolution and corrosion behavior of the AA6061 coating deposited by friction surfacing, J. Mater. Process. Technol. 291 (2020) 117005, doi:10.1016/j.jmatprotec.2020.117005.
[13] R. Damodaram, P. Rai, S. Cyril Joseph Daniel, R. Bauri, D. Yadav, Friction surfacing: a tool for surface crack repair, Surf. Coat. Technol. 422 (2021) 127482, doi:10.1016/j.surfcoat.2021.127482.
[14] H. Tokisue, K. Katoh, T. Asahina, T. Ushiyama, Mechanical properties of 5052/2017 dissimilar aluminum alloys deposit by friction surfacing, Mater. Trans. 47 (3) (2006) 874–882.
[15] J.C. Galvis, P.H.F. Oliveira, J.d.P. Martins, A.L.M.d. Carvalho, Assessment of process parameters by friction surfacing on the double layer deposition, Mater. Res. 21 (3) (2018) 321, doi:10.1590/1980-5373-mr-2018-0051.
[16] S. Krall, C. Baumann, H. Agiwal, F. Bleicher, F. Pfefferkorn, Investigation of multilayer coating of EN AW 6060–T66 using friction surfacing, J. Mach. Eng. 22(3). 10.36897/jme/147502.
[17] E.S. Abdelall, A.F. Al-Dwairi, S.M. Al-Raba'a, M. Eldakroury, Printing functional metallic 3D parts using a hybrid friction-surfacing additive manufacturing process, Prog. Addit. Manuf. 10 (3) (2021) 103, doi:10.1007/s40964-021-00193-3.
[18] J. Shen, S. Hanke, A. Roos, J.F. DosSantos, B. Klusemann, Fundamental study on additive manufacturing of aluminium alloys by friction surfacing layer deposition, in: 22nd International Conference on Material Forming, ESAFORM, 2019, doi:10.1063/1.5112691.
[19] L. Rath, Z. Kallien, A. Roos, J.F.d. Santos, B. Klusemann, Anisotropy and mechanical properties of dissimilar al additive manufactured structures generated by multi-layer friction surfacing, Int. J. Adv. Manuf. Technol. 117 (6) (2023) 371, doi:10.1007/s00170-022-10685-3.
[20] Z. Kallien, A. Roos, C. Knothe-Horstmann, B. Klusemann, Temperature-dependent mechanical behavior of aluminum AM structures generated via multi-layer friction surfacing, Mater. Sci. Eng., A 871C (2023) 144872, doi:10.1016/j.msea.2023.144872.
[21] M. Soujon, Z. Kallien, A. Roos, B. Zeller-Plumhoff, B. Klusemann, Fundamental study of multi-track friction surfacing deposits for dissimilar aluminum alloys with application to additive manufacturing, Mater. Des. 219 (5) (2022) 110786, doi:10.1016/j.matdes.2022.110786.
[22] D.Z. Avery, C. Cleek, B.J. Phillips, M. Rekha, R.P. Kinser, H. Rao, L. Brewer, P. Allison, J. Jordon, Evaluation of microstructure and mechanical properties of Al-Zn-Mg-Cu alloy repaired via additive friction stir deposition, J. Eng. Mater. Technol. 144 (3) (2022) 031003.
[23] M. Williams, T. Robinson, C. Williamson, R. Kinser, N. Ashmore, P. Allison, J. Jordon, Elucidating the effect of additive friction stir deposition on the resulting microstructure and mechanical properties of magnesium alloy WE43, Metals 11 (11) (2021) 1739, doi:10.3390/met11111739.
[24] B.A. Rutherford, D.Z. Avery, B.J. Phillips, H.M. Rao, K.J. Doherty, P.G. Allison, L.N. Brewer, J.B. Jordon, Effect of thermomechanical processing on fatigue behavior in solid-state additive manufacturing of Al-Mg-Si alloy, Metals 10 (7) (2020) 947, doi:10.3390/met10070947.
[25] J. Torzewski, K. Grzelak, M. Wachowski, R. Kosturek, Microstructure and low cycle fatigue properties of AA5083 H111 friction stir welded joint, Materials 13 (10) (2020) 2381, doi:10.3390/ma13102381.
[26] W. Abuzaid, R. Hawileh, J. Abdalla, Mechanical properties of strengthening 5083-H111 aluminum alloy plates at elevated temperatures, Infrastructures 6 (6) (2021) 87.
[27] K.K. Kumar, A. Kumar, M. Satyanarayana, Effect of friction stir welding parameters on the material flow, mechanical properties and corrosion behavior of dissimilar AA5083–AA6061 joints, Proc. Inst. Mech. Eng., Part C 236 (6) (2022) 2901–2917.
[28] U. Zerbst, M. Vormwald, R. Pippan, H.-P. Gänser, C. Sarrazin-Baudoux, M. Madia, About the fatigue crack propagation threshold of metals as a design criterion—A review, Eng. Fract. Mech. 153 (2016) 190–243, doi:10.1016/j.engfracmech.2015.12.002.
[29] G. Dovzhenko, S. Hanke, P. Staron, E. Maawad, A. Schreyer, M. Horstmann, Residual stresses and fatigue crack growth in friction surfacing coated Ti-6Al-4V sheets, J. Mater. Process. Technol. 262 (2018) 104–110, doi:10.1016/j.jmatprotec.2018.06.029.
[30] S.M. Bararpour, H. Jamshidi Aval, R. Jamaati, An experimental and theoretical investigation of thermo-mechanical issues in friction surfacing of Al-Mg aluminium alloys: material flow and residual stress, Model. Simul. Mater. Sci. Eng. 28 (3), doi:10.1088/1361-651X/ab6bff.
[31] S. Keller, M. Horstmann, N. Kashaev, B. Klusemann, Experimentally validated multi-step simulation strategy to predict the fatigue crack propagation rate in residual stress fields after laser shock peening, Int. J. Fatigue 124 (2019) 265–276, doi:10.1016/j.ijfatigue.2018.12.014.
[32] G. Pouget, A.P. Reynolds, Residual stress and microstructure effects on fatigue crack growth in AA2050 friction stir welds, Int. J. Fatigue 30 (3) (2008) 463–472, doi:10.1016/j.ijfatigue.2007.04.016.
[33] N. Zhu, D. Avery, Y. Chen, K. An, J. Jordon, P. Allison, L. Brewer, Residual stress distributions in AA6061 material produced by additive friction stir deposition, J. Mater. Eng. Perform. (2022) 1–10, doi:10.1007/s11665-022-07483-z.